Winter subglacial meltwater detected in Greenland Fjord

Karina Hansen[1], Nanna B. Karlsson[1,*], Penelope How[1], Ebbe Poulsen[2], John Mortensen[3], and Søren Rysgaard[2]

[1]Department of Glaciology and Climate, Geological Survey of Denmark and Greenland, Copenhagen, Denmark
[2]Arctic Research Centre, Department of Biology, Aarhus University, Aarhus, Denmark
[3]Greenland Climate Research Centre, Greenland Institute of Natural Resources, Nuuk, Greenland
[*]nbk@geus.dk

Abstract

The interaction between glacier fronts and ocean waters is one of the key uncertainties for projecting future ice mass loss. Direct observations at glacier fronts are sparse, but studies indicate that the magnitude and timing of freshwater fluxes are crucial in determining fjord circulation, ice frontal melt and ecosystem habitability. In particular, wintertime dynamics are severely understudied due to inaccessible conditions, leading to a bias towards summer observations. Here, we present in-situ observations of temperature and salinity acquired in late winter in Greenland at the front of a marine-terminating glacier and in surrounding fjords. Our observations indicate the existence of an anomalously fresh pool of water by the glacier front, suggesting that meltwater generated at the bed of the glacier discharges during winter. The results suggest that warm Atlantic water and nutrients are entrained at the glacier front, leading to enhanced frontal melt and increased nutrient levels. Our findings have implications for understanding the heat exchange between glacier fronts and ocean waters, glacier frontal melt rates, ocean mixing and currents, and biological production.

Main

In Greenland, marine-terminating glaciers release meltwater at depth, causing a mixing of buoyant meltwater and saline ocean water [1, 2]. The discharge of subglacial meltwater and subsequent mixing leads to an upwelling of deep fjord waters close to the glacier fronts, influencing the circulation in the fjord systems [3, 4]. The meltwater impacts glacial frontal melt [5, 6] and ice mélange melt [7], thereby modifying the mass loss from marine-terminating glaciers and consequently glacier contribution to future sea-level rise [8, 9]. The upwelling also impacts the influx and mixing of

nutrients [10, 11, 12], enhancing biological primary productivity and providing feeding grounds for fish and seabirds [13, 14].

Greenland fjords experience large seasonal variability in temperature and salinity [4, 15]. During the summer, subglacial meltwater, predominantly from surface runoff, has been observed in fjord waters as a layered structure below the surface layer [7]. In contrast, winter measurements of subglacial discharge into Greenland fjords are effectively unprecedented. Thus, the volume of winter subglacial discharge and its impact on fjord systems remains an open question [16], and model estimates of winter meltwater differ by orders of magnitude [5, 17, 18]. Measurements in Kangersuneq (in Nuup Kangerlua, West Greenland) revealed a considerable difference in temperature-salinity profiles between summer and winter, suggesting no noteworthy freshwater outflow from nearby glaciers during winter [1]. Studies of the Milne Fjord epishelf lake, northern Canada, report similar findings suggesting that winter freshwater discharge is negligible [19]. In contrast, studies from Svalbard fjords have found evidence of freshwater input during winter [20, 21] and early spring [22]. However, due to the shallow fjord depths (10s of metres), and consequently shallow grounding lines [21, 22], this meltwater is likely added directly into the fjord surface layers, implying that its effect on fjord circulation is separate from subglacial freshwater discharged at depth (100s metres).

However, due to the shallow fjord depths, this meltwater is likely added directly into the fjord surface layers, implying that its effect on fjord circulation is separate from subglacial freshwater discharged at depth.

In contrast to observations, theoretical estimates of winter freshwater volumes indicate that subglacial meltwater discharges at depth into Greenland fjords all year round [17, 18, 23]. However, fjord circulation models disagree on the importance of winter discharge for heat and water exchange [24, 25]. In the absence of other freshwater fluxes, the winter discharge of glacial meltwater may have a pronounced influence on fjord dynamics, but its impact will depend on water volumes and fjord/glacier settings [16]. This underscores the complexity of bathymetry and heat exchange dynamics between the shelf and marine-terminating glaciers within individual fjords. Finally, the fast-changing Arctic climate may already be causing shifts in wintertime conditions, highlighting the urgency for a better understanding of wintertime dynamics. To our knowledge, our study is the first to measure and document the existence of subglacial freshwater in a Greenland fjord during winter, shedding light on a hitherto undocumented process.

In-situ observations of temperature and salinity

During a dedicated field season in March 2023, we carried out in-situ observations of water properties at Eqalorutsit Kangilliit Sermiat (at times referred to as Qajuutaap) and neighbouring fjords (Fig. 1). Eqalorutsit Kangilliit Sermiat is one of the largest marine-terminating glaciers in South Greenland (its drainage basin and discharge rates are only matched by neighbouring Eqalorutsit Killiit Sermiat [26, 23]) with an ice front grounded several hundred metres below sea level and a grounding line depth that in places exceeds 400 m below sea level [27]. The glacier discharges into an eastern branch of Sermilik Fjord, which forms the inner part of Ikersuaq Fjord (formerly Bredefjord). The fjord depth ranges from 60 m to 600 m below sea level, but bathymetric maps in the middle part of

the fjord are highly uncertain due to a lack of in-situ observations.

To retrieve temperature and salinity measurements, we developed and deployed a novel uncrewed aerial vehicle (UAV) solution (Fig. 2). Dense ice mélange has prevented previous studies from acquiring measurements in glacial fjords during winter, and the UAV was crucial to our success. The UAV platform consists of a modified kit helicopter with an onboard autonomous winch and a commercial CTD (conductivity, temperature, and depth) sensor payload (see [28] and methods). Its maximum total flight time is 24 minutes, allowing for measurements to be collected up to a distance of 6 km although our measurements were acquired less than 1.5 km from the deployment sites. We carried out additional CTD deployments in front of Eqalorutsit Kangilliit Sermiat, where flat, walkable fjord ice enabled us to drill two holes manually in the ice (Fig. 3). The heavy fjord-ice conditions in neighbouring Tunulliarfik Fjord also made it possible to drill a hole manually and make CTD casts.

Temperature and salinity data were derived from the CTD profiles, and salinity was calculated using the practical salinity scale (PSS-78). In the upper 30 m, temperature and salinity conditions cluster in three characteristic patterns (Fig. 4): the coldest and freshest conditions were found near the glacier front (St. 1 and 2, orange and red lines, respectively), transitioning to slightly warmer and saltier water in the ice mélange (St. 3, 4, 5, 6, rose, magenta, pink, and blue lines, respectively) and Sermilik fjord (St. 7, turquoise lines). Compared to these measurements, conditions in Tunulliarfik fjord (St. 8, yellow line) are warmer and saltier, indicating that coastal water modifies the fjord waters. Below 40 m depth, measurements closest to the glacier front (St. 1 and 2) reach salinity levels similar to those in Tunulliarfik fjord (St. 8). For context, we include summer measurements from the OMG (Oceans Melting Greenland) project [29, 30] and from the Greenland Institute of Natural Resources (GINR) (Fig. 4, brown lines).

In the T-S-diagram (Fig. 4c), St. 1 and 2 measurements show a two-minima temperature profile (black arrows). Previous studies have interpreted two-minima temperature profiles as subglacial discharge [1, 7]. In contrast, two-minima temperature profiles are not seen in our CTD observations from the ice mélange (St. 3-6) or Sermilik fjord (St. 7). The down-fjord observations (St. 3-6) display a halocline layer (15-38 m depth) in the T-S-diagram that follows a melt line with an observed slope of 2.5°C per salinity unit, which corresponds to the Gade-slope [31]. According to the Gade model [31], the mixing of melted glacial ice with seawater appears as a straight line in a T-S-diagram with a slope of about 2.5°C per salinity unit. Thus, the down-fjord observations indicate that the freshening can be explained solely by the melting of ice mélange and stranded icebergs, while the freshening observed at St. 1 and 2 is caused by a mix of melt from ice mélange and icebergs, and subglacial discharge. Notably, measurements from St. 1 and 2 follow the same T-S-line as water in Tunulliarfik fjord (St. 8), indicating an influence from coastal water.

Fig. 4 also includes a rare winter observation from Nuup Kangerlua in West Greenland acquired $\sim$ 4 km from the glacier front of Kangiata Nunaata Sermia (black line, referred to as GF10099 [1]). A halocline layer (below 17 m depth) caused by melting of the ice mélange can be seen in our down-fjord observations (St. 3-8) and in GF10099. Comparison with our St. 1 and 2 measurements highlights the novelty of our observations. Where the surface layer temperature of GF10099 follows the freezing line, St. 1 and 2 profiles do not reach the freezing point and have local temperature

minima, showing a likely input of warmer waters such as a mixture of ambient deep fjord waters and subglacial meltwater discharge meltwater. Based on our observations, we suggest that 1) meltwater enters the fjord subglacially from Eqalorutsit Kangilliit Sermiat, freshening the surface layer and 2) the meltwater accumulates at the glacier front under the mélange in a "fresh surface pool of water" (Fig. 3) similar to reported epishelf lakes [19].

Freshwater volumes and sources

To our knowledge, our study is the first to document the existence of subglacial meltwater in a Greenland fjord during winter and to report evidence of upwelling at depth. The two-minima signal in our data is not as strong as observed during summer conditions (brown lines, Fig. 4, also [4]), indicating that the subglacial discharge may not be substantial. The fact that the freshwater pool is spatially confined is the likely reason why it has not been observed by previous studies, as measurements in those studies were retrieved 4 km [1] and 6 km [32] from the glacier front compared to our measurements that were 1 km (St. 1), 1.7 km (St. 2) and 5 km (St. 3) from the front.

Subglacial water may have different provenances. During summer, subglacially discharged water derives predominantly from surface meltwater that enters the subglacial system via moulins and crevasses [33]. During winter, in the absence of surface melt, the origin of the water is less clear. We suggest that the observed pool of meltwater originates from basal melting, that is, from melting at the interface between ice and bedrock. The basal conditions of the Greenland ice sheet are not well known, but estimates indicate that large parts of the ice sheet's base are at the melting point [34]. Studies suggest that basal melt is predominantly caused by heat from friction and geothermal flux [17, 35], and therefore, basal melt discharges during all seasons, making basal meltwater a potential source of wintertime freshwater.

Potential freshwater sources include surface melt and glacier-lake drainage events. Here, we outline why we discard these two meltwater sources as explanations for our measurements. Firstly, while large volumes of surface meltwater enter Sermilik Fjord in the summertime, the winter surface melt volume is orders of magnitude smaller due to low air temperatures (see Fig. S1). We estimate the likely surface melt using an improved Positive Degree Day model [36] and in-situ measurements from the PROMICE Automatic Weather Stations (AWS) [37] (see Fig. 1 and methods). Our results indicate that surface melt occurred for two days in early March (see Fig. S2). Only the lowest-elevation AWS experienced surface melt with daily melt rates of 5.6 mm and 6.4 mm on the 2nd and 3rd of March, respectively (three weeks before our measurements began). Given the small volume of meltwater generated, we posit that the water is unlikely to have penetrated to the bed of the glacier and that the majority of the water was retained and refrozen close to the ice surface, either in the broken and weathered bare-ice surface or in snow pockets [38]. This is supported by observational evidence of refrozen ice, snow pockets and dry crevasses at the glacier margin (Fig. S3).

While we discard recent surface melt as a potential source of freshwater, a delayed release of surface meltwater generated during the previous melt season could contribute to the observed freshwater signal. The travel time of meltwater in the Greenland subglacial system is poorly constrained; however, numerous studies (as summarised in [39]) have found evidence that the subglacial system

drains highly efficiently, indicating an overall limited storage capacity. This is supported by a recent study that used measurements of shifts in the Greenland bedrock to estimate that the average water storage time in South Greenland is 31±12 days [40]. Local topography may further promote surface water storage by pooling water into subglacial lakes. For example, evidence of winter meltwater from a land-terminating glacier in Greenland [41] was found upstream of an area previously identified as a potential area for subglacial water storage [42]. However, no subglacial lakes have been identified in our study area [43]. Lacking isotope measurements, we cannot disentangle surface meltwater from basal meltwater and it is possible that our observations represent a mix of both meltwater sources.

A second freshwater source is the drainage of ice-marginal lakes. Thus, we investigated 21 lakes that share a margin with the glacier's catchment area (mapped in 2017 [44]). Between January and April 2023, five of the 21 ice-marginal lakes around the lateral margins of Eqalorutsit Kangilliit Sermiat could be identified. Little is known about the dynamics of these lakes; however, satellite images suggest that their areas varied insignificantly during our period of interest and there is no evidence of glacial lake outburst floods or full drainage events during this period (see methods).

Other sources of freshwater at glacier fronts include melting of the glacier front itself. The frontal melt contribution to the freshwater budget of fjords is unresolved and recent laboratory studies suggest that frontal melt may be underestimated in models [45]. Nevertheless, observations in a Greenland fjord showed that the contribution from frontal melt is minor due to the small front surface compared to the ice mélange surface [7]. Importantly, meltwater originating from frontal melt will follow the Gade slope; therefore, if the freshwater signal consisted of frontal meltwater only, we would not observe a two-minima temperature profile.

Our study is the first to successfully measure meltwater linked to basal meltwater at a glacier front as opposed to precipitation or surface melt [20, 41]. The estimated monthly basal melt of Eqalorutsit Kangilliit Sermiat is 3.8×10^6 m^3 corresponding to 2 % of the glacier's annual mass loss [23]. This estimate is highly uncertain, and we leverage our CTD observations to evaluate the amount of freshwater necessary to cause the observed freshening. Our results indicate a freshwater volume corresponding to 2.4×10^5 m^3 (see methods). This estimate includes all sources that contribute to freshening the water at the front, including meltwater from the glacier front and the delayed release of surface meltwater, and it should, therefore, be considered an upper bound. Nevertheless, our estimate is an order of magnitude lower than the theoretically estimated monthly basal melt. We suggest several reasons for this discrepancy that are not mutually exclusive. Firstly, the source area for the basal meltwater is reconstructed based on surface and bed topography, where the latter has uncertainties upwards of 300 m [27]. Therefore, the source area may be smaller than estimated, lowering the modelled basal meltwater volume discharging at the glacier front. Secondly, studies suggest that the subglacial system can shut down during winter [46], blocking the transport of basal meltwater from upstream parts of the glacier basin. This potential disconnection between parts of the subglacial system may be highly dependent on ice-flow velocities and the glacier's topographic setting. Finally, our Station 1 and 2 measurements were acquired in a small bay a few kilometres east of where the glacier plume emerges in the summer. If it had been possible to get closer to the plume's likely central outflow, we might have seen a stronger freshwater signal.

Impacts of winter meltwater discharge

Our measurements indicate that basal meltwater released subglacially during winter modifies near-glacier water properties and influences processes controlling ice/fjord interactions, fjord dynamics and ecosystems. Modelling studies of summer plumes [47] have shown that upwelling of Atlantic Water driven by plumes may substantially warm near-glacier waters at intermediate depth, affecting the distribution and magnitude of frontal melt. We suggest that winter discharge will have a similar effect, i.e., enhanced mixing and entrainment of ambient water at the glacial front. Ambient water temperatures above 0°C, typically from Atlantic Water, will accelerate frontal melting. Conversely, for glaciers terminating in water with ambient temperatures below 0°C, winter discharge may promote refreezing and frazil ice formation in the fjord [48]. Thus, glaciers in contact with warmer waters, such as those in Southwest Greenland [49], are especially vulnerable to the effects of winter discharge, and an increase in winter freshwater would lead to increased frontal melt. However, there is a lack of understanding regarding the seasonal variation of water mass properties near glaciers and subglacial discharge outside the summer months [16], and more work is needed to include this effect in projections of future glacier mass loss from oceanic forcing, e.g., [9]. Thus, our findings underscore the urgent need to understand the role and impact of winter subglacial discharge on fjord dynamics.

The winter subglacial discharge from Eqalorutsit Kangilliit Sermiat likely replenishes nutrients in the surface waters, thereby readying the system for expansive primary production during spring when the ice mélange breaks up. Hence, winter subglacial discharge in the inner parts of fjords may play a more critical role in priming the spring phytoplankton production than previously anticipated. It has been reported that the spring bloom in a marine-terminating glacier fjord will be triggered by out-fjord winds and coastal inflows driving an upwelling in the inner part of the fjord, hereby supplying nutrient-rich water to the surface layer [50]. Our observations suggest that winter subglacial discharge may entrain nutrients from deeper waters and accumulate them in a surface pool of water beneath the ice mélange near the glacier front. As a result, favourable conditions for a spring phytoplankton bloom are expected to establish when the mélange breaks up as observed further north in the Nuup Kangerlua fjord system [51]. It is noteworthy that the spring bloom might not occur directly in front of the glacier but further out in the fjord, as the nutrient pool will track the drifting ice pushed by prevailing winds from the northeast during spring (see observed wind directions in Fig. S6). This further underscores the seasonal significance of marine-terminating glaciers in stimulating primary production.

Observations and models suggest that subglacial discharge causes fjord circulation patterns leading to a renewal of fjord basin waters over seasonal time scales [2, 52]. Although melt from icebergs and ice mélange probably dominates the winter freshwater budget for most ice-filled fjords [53], any inflow of glacial freshwater may be of physical and biogeochemical significance [16]. Nevertheless, most fjord circulation models focus on summertime dynamics aiming to understand processes occurring during the peak meltwater season [54, 55]. In the near future, increasing Arctic temperatures are likely to lead to a speed-up of Greenland glaciers [56] and consequently an increase in basally generated meltwater due to increased friction [35] and thereby also an increased winter freshwater

discharge. Thus, there is an urgent need to understand the role and impact of winter subglacial discharge on fjord dynamics.

Our unique observations of winter subglacial discharge highlight the importance of this severely understudied freshwater source and demonstrate the potential of UAV-supported observations during the Arctic winter. The potentially disproportionately large influence of winter subglacial discharge on fjord waters when considering its comparatively small volume, coupled with its ability to enhance spring primary production, emphasises the significant impact marine-terminating glaciers can exert on fjord waters, fjord circulation, and ecosystem productivity, with consequences for fisheries in the coastal zone surrounding Greenland.

Acknowledgements

This work was supported by a Villum Experiment project to NBK from the Villum Foundation (project no. 40858). Further support was provided by PROMICE, funded by the Geological Survey of Denmark and Greenland (GEUS) and the Danish Ministry of Climate, Energy and Utilities under the Danish Cooperation for Environment in the Arctic (DANCEA), conducted in collaboration with DTU Space (Technical University of Denmark) and Asiaq Greenland Survey. The development of the UAV was supported by Aage V Jensens Foundations to the project "Greenland gradients Flagship project". PH was supported by a European Space Agency Living Planet Fellowship (4000136382/21/I-DT-lr) entitled "Examining Greenland's Ice Marginal Lakes under a Changing Climate". We thank Baptiste Vandecrux (GEUS) for advice and insightful discussions on calculating surface melt. The skilled and patient employees of the Department of Biology mechanical and electrical workshops are acknowledged for their significant contributions during the design and build of the ARC-AWS. We acknowledge the helpful community of ArduPilot and Bill Geyer for support and guidance during UAV development. Egon R. Frandsen is acknowledged for logistical support during fieldwork. We thank the pilots from SERMEQ helicopters for their support and enthusiasm during the 2023 fieldwork.

Author contributions statement

NBK conceived of the study in collaboration with SR. KH managed the project and planned the fieldwork campaign. EP developed the UAV solution with input from SR. EP, SR, KH and NBK collected the data and analysed it with input from JM. KH calculated surface melt rates. PH compiled and analysed the ice-marginal lake observations. NBK, SR and KH led the writing of the article with contributions from all authors. NBK and SR acquired the funding for the work. All authors reviewed the manuscript.

Competing interests

The authors declare that they have no competing interests.

Figure captions

Figure 1: *Overview map of our study area and measurement sites. The locations of our measurement stations are indicated with coloured circles, where measurements acquired by our Uncrewed Autonomous Vehicle (UAV) are outlined with a thick black line. Measurements from the OMG project (Oceans Melting Greenland [30]) and the Greenland Institute of Natural Resources (GINR, KR23034) are indicated with a brown diamond and brown triangle, respectively. PROMICE (Programme for Monitoring of the Greenland Ice Sheet) automatic weather stations (AWS) are marked with black stars. Ice marginal lakes are outlined with turquoise [44], and the ice sheet is coloured grey with 200 m surface topography contours in dashed grey lines from [27, 57]. The background image is optical satellite data from Sentinel 2 (Copernicus Sentinel data, processed by the European Space Agency) from the 27th of March 2023. The location of the map is indicated on the overview map in red, also showing 500 m surface topography contours [27, 57] and surface velocities in blue [58].*

Figure 2: *Photographs of our UAV platform. (a) Complete UAV platform with CTD payload extended. (b) UAV during profiling in a narrow section of open water created by a seal. The seal hole in the sea ice is smaller (approximately 0.5 m) than the flooded surface area. Note the line extending from the UAV to the submerged CTD instrument. The UAV platform has a length of 1.145 m and a rotor diameter of 1.455 m. Photos are from two different deployments, courtesy of Lars Ostenfeld and the authors.*

Figure 3: *Schematic of the measurement conditions for the UAV and the manual drill in glacier/ice melange/fjord system. (a) and (b) show enlarged versions of our measurement techniques.*

Figure 4: *In-situ measurements from the CTD sensors. The figures show CTD profiles of (a) temperature and (b) salinity, and (c) the corresponding T-S-diagram (locations are shown in Fig. 1). Observations from GINR (KR23034, July 2023) and the OMG project (August 2018) are shown as brown lines. Dotted lines indicate measurements from neighbouring Tunulliarfik fjord. A GINR winter observation from Nuup Kangerlua in West Greenland is shown in black (GF10099, April 2010). A Gade-slope of 2.5° C per salinity unit is indicated with thick grey. The freezing point line of seawater is shown as a dashed-dotted grey line. Black arrows indicate the two-temperature minima seen in St. 1 and 2 data.*

References

[1] Mortensen, J., Bendtsen, J., Motyka, R. J., Lennert, K., Truffer, M., Fahnestock, M. & Rysgaard, S. On the seasonal freshwater stratification in the proximity of fast-flowing tidewater outlet glaciers in a sub-Arctic sill fjord. *Journal of Geophysical Research: Oceans* **118**, 1382–1395 (2013).

[2] Carroll, D., Sutherland, D. A., Shroyer, E. L., Nash, J. D., Catania, G. A. & Stearns, L. A. Modeling Turbulent Subglacial Meltwater Plumes: Implications for Fjord-Scale Buoyancy-Driven Circulation. *Journal of Physical Oceanography* 2169–2185 (2015).

[3] Straneo, F. & Cenedese, C. The Dynamics of Greenland's Glacial Fjords and Their Role in Climate. *Annual Review of Marine Science* **7**, 89–112 (2015).

[4] Mortensen, J., Bendtsen, J., Lennert, K. & Rysgaard, S. Seasonal variability of the circulation system in a west Greenland tidewater outlet glacier fjord, Godthåbsfjord (64 N). *Journal of Geophysical Research: Earth Surface* **119**, 2591–2603 (2014).

[5] Rignot, E., Xu, Y., Menemenlis, D., Mouginot, J., Scheuchl, B., Li, X., Morlighem, M., Seroussi, H., den Broeke, M. v., Fenty, I. *et al.* Modeling of ocean-induced ice melt rates of five west Greenland glaciers over the past two decades. *Geophysical Research Letters* **43**, 6374–6382 (2016).

[6] Jackson, R., Nash, J., Kienholz, C., Sutherland, D., Amundson, J., Motyka, R., Winters, D., Skyllingstad, E. & Pettit, E. Meltwater intrusions reveal mechanisms for rapid submarine melt at a tidewater glacier. *Geophysical Research Letters* **47**, e2019GL085335 (2020).

[7] Mortensen, J., Rysgaard, S., Bendtsen, J., Lennert, K., Kanzow, T., Lund, H. & Meire, L. Subglacial discharge and its down-fjord transformation in West Greenland fjords with an ice mélange. *Journal of Geophysical Research: Oceans* **125**, e2020JC016301 (2020).

[8] Beckmann, J., Perrette, M., Beyer, S., Calov, R., Willeit, M. & Ganopolski, A. Modeling the response of Greenland outlet glaciers to global warming using a coupled flow line–plume model. *The Cryosphere* **13**, 2281–2301 (2019). URL `https://www.the-cryosphere.net/13/2281/2019/`.

[9] Slater, D. A., Felikson, D., Straneo, F., Goelzer, H., Little, C. M., Morlighem, M., Fettweis, X. & Nowicki, S. Twenty-first century ocean forcing of the Greenland ice sheet for modelling of sea level contribution. *The Cryosphere* **14**, 985–1008 (2020).

[10] Meire, L., Mortensen, J., Meire, P., Juul-Pedersen, T., Sejr, M. K., Rysgaard, S., Nygaard, R., Huybrechts, P. & Meysman, F. J. Marine-terminating glaciers sustain high productivity in Greenland fjords. *Global Change Biology* **23**, 5344–5357 (2017).

[11] Kanna, N., Sugiyama, S., Ohashi, Y., Sakakibara, D., Fukamachi, Y. & Nomura, D. Upwelling of Macronutrients and Dissolved Inorganic Carbon by a Subglacial Freshwater Driven Plume

in Bowdoin Fjord, Northwestern Greenland. *Journal of Geophysical Research: Biogeosciences* **123**, 1666–1682 (2018).

[12] Hopwood, M. J., Carroll, D., Dunse, T., Hodson, A., Holding, J. M., Iriarte, J. L., Ribeiro, S., Achterberg, E. P., Cantoni, C., Carlson, D. F., Chierici, M., Clarke, J. S., Cozzi, S., Fransson, A., Juul-Pedersen, T., Winding, M. H. & Meire, L. Review article: How does glacier discharge affect marine biogeochemistry and primary production in the Arctic? *Cryosphere* **14**, 1347–1383 (2020).

[13] Hopwood, M. J., Carroll, D., Browning, T. J., Meire, L., Mortensen, J., Krisch, S. & Achterberg, E. P. Non-linear response of summertime marine productivity to increased meltwater discharge around Greenland. *Nature Communications* **9** (2018).

[14] Nishizawa, B., Kanna, N., Abe, Y., Ohashi, Y., Sakakibara, D., Asaji, I., Sugiyama, S., Yamaguchi, A. & Watanuki, Y. Contrasting assemblages of seabirds in the subglacial meltwater plume and oceanic water of Bowdoin Fjord, northwestern Greenland. *ICES Journal of Marine Science* **77**, 711–720 (2019). URL `https://doi.org/10.1093/icesjms/fsz213`. `https://academic.oup.com/icesjms/article-pdf/77/2/711/32881925/fsz213.pdf`.

[15] Jackson, R. H., Straneo, F. & Sutherland, D. A. Externally forced fluctuations in ocean temperature at Greenland glaciers in non-summer months. *Nature Geoscience* **7**, 503–508 (2014).

[16] Vonnahme, T. R., Nowak, A., Hopwood, M. J., Meire, L., Søgaard, D. H., Krawczyk, D., Kalhagen, K. & Juul-Pedersen, T. Impact of winter freshwater from tidewater glaciers on fjords in Svalbard and Greenland; A review. *Progress in Oceanography* **219**, 103144 (2023). URL `https://www.sciencedirect.com/science/article/pii/S0079661123001878`.

[17] Cook, S. J., Swift, D. A., Kirkbride, M. P., Knight, P. G. & Waller, R. I. The empirical basis for modelling glacial erosion rates. *Nature Communications* **11** (2020).

[18] Sommers, A., Meyer, C., Morlighem, M., Rajaram, H., Poinar, K., Chu, W. & Mejia, J. Subglacial hydrology modeling predicts high winter water pressure and spatially variable transmissivity at Helheim Glacier, Greenland. *Journal of Glaciology* 1–13 (2023).

[19] Hamilton, A. K., Mueller, D. & Laval, B. E. Ocean Modification and Seasonality in a Northern Ellesmere Island Glacial Fjord Prior to Ice Shelf Breakup: Milne Fiord. *Journal of Geophysical Research: Oceans* **126**, e2020JC016975 (2021). E2020JC016975 2020JC016975.

[20] Fransson, A., Chierici, M., Nomura, D., Granskog, M. A., Kristiansen, S., Martma, T. & Nehrke, G. Effect of glacial drainage water on the CO2 system and ocean acidification state in an Arctic tidewater-glacier fjord during two contrasting years. *Journal of Geophysical Research: Oceans* **120**, 2413–2429 (2015).

[21] Marchenko, A. V., Morozov, E. G. & Marchenko, N. A. Supercooling of Seawater Near the Glacier Front in a Fjord. *Earth Science Research* **6**, 97–108 (2017).

[22] Vonnahme, T. R., Persson, E., Dietrich, U., Hejdukova, E., Dybwad, C., Elster, J., Chierici, M. & Gradinger, R. Early spring subglacial discharge plumes fuel under-ice primary production at a Svalbard tidewater glacier. *The Cryosphere* **15**, 2083–2107 (2021).

[23] Karlsson, N. B., Mankoff, K. D., Solgaard, A. M., Larsen, S. H., How, P. R., Fausto, R. S. & Sørensen, L. S. A data set of monthly freshwater fluxes from the Greenland ice sheet's marine-terminating glaciers on a glacier–basin scale 2010–2020. *GEUS Bulletin* **53** (2023). URL `https://geusbulletin.org/index.php/geusb/article/view/8338`.

[24] Fraser, N. J., Inall, M. E., Magaldi, M. G., Haine, T. W. N. & Jones, S. C. Wintertime Fjord-Shelf Interaction and Ice Sheet Melting in Southeast Greenland. *Journal of Geophysical Research: Oceans* **123**, 9156–9177 (2018).

[25] Hager, A. O., Sutherland, D. A. & Slater, D. A. Local forcing mechanisms challenge parameterizations of ocean thermal forcing for Greenland tidewater glaciers. *The Cryosphere* **18**, 911–932 (2024).

[26] Mankoff, K. D., Noël, B., Fettweis, X., Ahlstrøm, A. P., Colgan, W., Kondo, K., Langley, K., Sugiyama, S., van As, D. & Fausto, R. S. Greenland liquid water discharge from 1958 through 2019. *Earth System Science Data* **12**, 2811–2841 (2020).

[27] Morlighem, M., Williams, C. N., Rignot, E., An, L., Arndt, J. E., Bamber, J. L., Catania, G., Chauché, N., Dowdeswell, J. A., Dorschel, B., Fenty, I., Hogan, K., Howat, I., Hubbard, A., Jakobsson, M., Jordan, T. M., Kjeldsen, K. K., Millan, R., Mayer, L., Mouginot, J., Noël, B. P. Y., O'Cofaigh, C., Palmer, S., Rysgaard, S., Seroussi, H., Siegert, M. J., Slabon, P., Straneo, F., van den Broeke, M. R., Weinrebe, W., Wood, M. & Zinglersen, K. B. BedMachine v3: Complete Bed Topography and Ocean Bathymetry Mapping of Greenland From Multibeam Echo Sounding Combined With Mass Conservation. *Geophysical Research Letters* **44**, 11,051–11,061 (2017).

[28] Poulsen, E., Rysgaard, S., Hansen, K. & Karlsson, N. B. Uncrewed aerial vehicle with onboard winch system for rapid, cost-effective, and safe oceanographic profiling in hazardous and inaccessible areas. *HardwareX* **18**, e00518 (2024).

[29] OMG. 2020. OMG CTD Conductivity Temperature Depth. Ver. 1. Dataset accessed [2023-12-18].

[30] Fenty, I., Willis, J. K., Khazendar, A., Dinardo, S., Forsberg, R., Fukumori, I., Holland, D., Jakobsson, M., Moller, D., Morison, J. *et al.* Oceans Melting Greenland: Early results from NASA's ocean-ice mission in Greenland. *Oceanography* **29**, 72–83 (2016).

[31] Gade, H. G. Melting of Ice in Sea Water: A Primitive Model with Application to the Antarctic Ice Shelf and Icebergs. *Journal of Physical Oceanography* **9**, 189 – 198 (1979).

[32] Straneo, F., Curry, R. G., Sutherland, D. A., Hamilton, G. S., Cenedese, C., Våge, K. & Stearns, L. A. Impact of fjord dynamics and glacial runoff on the circulation near Helheim Glacier. *Nature Geoscience* **4**, 322–327 (2011).

[33] Hoffman, M. J., Andrews, L. C., Price, S. F., Catania, G. A., Neumann, T. A., Lüthi, M. P., Gulley, J., Ryser, C., Hawley, R. L. & Morriss, B. Greenland subglacial drainage evolution regulated by weakly connected regions of the bed. *Nature Communications* **9** (2016).

[34] MacGregor, J. A., Chu, W., Colgan, W. T., Fahnestock, M. A., Felikson, D., Karlsson, N. B., Nowicki, S. M. J. & Studinger, M. GBaTSv2: a revised synthesis of the likely basal thermal state of the Greenland Ice Sheet. *The Cryosphere* **16**, 3033–3049 (2022).

[35] Karlsson, N. B., Solgaard, A. M., Mankoff, K. D., Gillet-Chaulet, F., MacGregor, J. A., Box, J. E., Citterio, M., Colgan, W. T., Larsen, S. H., Kjeldsen, K. K., Korsgaard, N. J., Benn, D. I., Hewitt, I. J. & Fausto, R. S. A first constraint on basal melt-water production of the Greenland ice sheet. *Nature Communications* **12** (2021).

[36] Tsai, V. C. & Ruan, X. A simple physics-based improvement to the positive degree day model. *Journal of Glaciology* **64**, 661–668 (2018).

[37] Fausto, R., Mernild, S., Hasholt, B., Ahlstrøm, A. & Knudsen, N. Modeling suspended sediment concentration and transport, Mittivakkat glacier, southeast Greenland. *Arctic, Antarctic, and Alpine Research* **44**, 306–318 (2012).

[38] Cooper, M. G., Smith, L. C., Rennermalm, A. K., Miège, C., Pitcher, L. H., Ryan, J. C., Yang, K. & Cooley, S. W. Meltwater storage in low-density near-surface bare ice in the Greenland ice sheet ablation zone. *The Cryosphere* **12**, 955–970 (2018). URL `https://tc.copernicus.org/articles/12/955/2018/`.

[39] Nienow, P. W., Sole, A. J., Slater, D. A. & Cowton, T. R. Recent Advances in Our Understanding of the Role of Meltwater in the Greenland Ice Sheet System. *Current Climate Change Reports* **3**, 330–344 (2017).

[40] Ran, J., Ditmar, P., van den Broeke, M. R., Liu, L., Klees, R., Khan, S. A., Moon, T., Li, J., Bevis, M., Zhong, M., Fettweis, X., Liu, J., Noël, B., Shum, C. K., Chen, J., Jiang, L. & van Dam, T. Vertical bedrock shifts reveal summer water storage in Greenland ice sheet. *Nature* **635**, 108–113 (2024).

[41] Pitcher, L. H., Smith, L. C., Gleason, C. J., Miège, C., Ryan, J. C., Hagedorn, B., van As, D., Chu, W. & Forster, R. R. Direct Observation of Winter Meltwater Drainage From the Greenland Ice Sheet. *Geophysical Research Letters* **47**, e2019GL086521 (2020).

[42] Chu, W., Schroeder, D. M., Seroussi, H., Creyts, T. T., Palmer, S. J. & Bell, R. E. Extensive winter subglacial water storage beneath the Greenland Ice Sheet. *Geophysical Research Letters* **43**, 12,484–12,492 (2016).

[43] Livingstone, S. J., Li, Y., Rutishauser, A., Sanderson, R. J., Winter, K., Mikucki, J. A., Björnsson, H., Bowling, J. S., Chu, W., Dow, C. F., Fricker, H. A., McMillan, M., Ng, F. S. L., Ross, N., Siegert, M. J., Siegfried, M. & Sole, A. J. Subglacial lakes and their changing role in a warming climate. *Nature Reviews Earth & Environment* **3**, 106–124 (2022).

[44] How, P., Messerli, A., Mätzler, E., Santoro, M., Wiesmann, A., Caduff, R., Langley, K., Bojesen, M. H., Paul, F., Kääb, A. *et al.* Greenland-wide inventory of ice marginal lakes using a multi-method approach. *Scientific reports* **11**, 4481 (2021).

[45] Wengrove, M. E., Pettit, E. C., Nash, J. D., Jackson, R. H. & Skyllingstad, E. D. Melting of glacier ice enhanced by bursting air bubbles. *Nature Geoscience* **16**, 871–876 (2014).

[46] Flowers, G. E. Hydrology and the future of the Greenland Ice Sheet. *Nature Communications* **9** (2018).

[47] Cowton, T. R., Slater, D. A. & Inall, M. E. Subglacial-Discharge Plumes Drive Widespread Subsurface Warming in Northwest Greenland's Fjords. *Geophysical Research Letters* **50**, e2023GL103801 (2023).

[48] Rooijakkers, F. J., Poulsen, E., Ruiz-Castillo, E. & Rysgaard, S. Evidence suggesting frazil ice crystal formation at the front of Hisinger Glacier in Dickson Fjord, Northeast Greenland. *EGUsphere* **2024**, 1–20 (2024). URL `https://egusphere.copernicus.org/preprints/2024/egusphere-2024-2168/`.

[49] Rysgaard, S., Boone, W., Carlson, D., Sejr, M. K., Bendtsen, J., Juul-Pedersen, T., Lund, H., Meire, L. & Mortensen, J. An Updated View on Water Masses on the pan-West Greenland Continental Shelf and Their Link to Proglacial Fjords. *Journal of Geophysical Research: Oceans* **125**, e2019JC015564 (2020).

[50] Meire, L., Mortensen, J., Rysgaard, S., Bendtsen, J., Boone, W., Meire, P. & Meysman, F. J. Spring bloom dynamics in a subarctic fjord influenced by tidewater outlet glaciers (Godthåbsfjord, SW Greenland). *Journal of Geophysical Research: Biogeosciences* **121**, 1581–1592 (2016).

[51] Meire, L., Paulsen, M. L., Meire, P., Rysgaard, S., Hopwood, M. J., Sejr, M. K., Stuart-Lee, A., Sabbe, K., Stock, W. & Mortensen, J. Glacier retreat alters downstream fjord ecosystem structure and function in Greenland. *Nature Geoscience* (2023).

[52] Carroll, D., Sutherland, D. A., Shroyer, E. L., Nash, J. D., Catania, G. A. & Stearns, L. A. Subglacial discharge-driven renewal of tidewater glacier fjords. *Journal of Geophysical Research: Oceans* **122**, 6611–6629 (2017).

[53] Moon, T., Sutherland, D. A., Carroll, D., Felikson, D., Kehrl, L. & Straneo, F. Subsurface iceberg melt key to Greenland fjord freshwater budget. *Nature Geoscience* **11** (2018).

[54] Cape, M. R., Straneo, F., Beaird, N., Bundy, R. M. & Charette, M. A. Nutrient release to oceans from buoyancy-driven upwelling at Greenland tidewater glaciers. *Nature Geoscience* **12** (2019).

[55] Torsvik, T., Albretsen, J., Sundfjord, A., Kohler, J., Sandvik, A. D., Skarðhamar, J., Lindbäck, K. & Everett, A. Impact of tidewater glacier retreat on the fjord system: Modeling present and future circulation in Kongsfjorden, Svalbard. *Estuarine, Coastal and Shelf Science* **220**, 152–165 (2019).

[56] Goelzer, H., Nowicki, S., Payne, A., Larour, E., Seroussi, H., Lipscomb, W. H., Gregory, J., Abe-Ouchi, A., Shepherd, A., Simon, E., Agosta, C., Alexander, P., Aschwanden, A., Barthel, A., Calov, R., Chambers, C., Choi, Y., Cuzzone, J., Dumas, C., Edwards, T., Felikson, D., Fettweis, X., Golledge, N. R., Greve, R., Humbert, A., Huybrechts, P., Clec'H, S. L., Lee, V., Leguy, G., Little, C., Lowry, D., Morlighem, M., Nias, I., Quiquet, A., Rückamp, M., Schlegel, N. J., Slater, D. A., Smith, R., Straneo, F., Tarasov, L., Wal, R. V. D. & Broeke, M. V. D. The future sea-level contribution of the Greenland ice sheet: A multi-model ensemble study of ISMIP6. *Cryosphere* **14**, 3071–3096 (2020).

[57] Morlighem, M. e. a. IceBridge BedMachine Greenland, Version 5 (2022). URL `https://nsidc.org/data/IDBMG4/versions/5`.

[58] Solgaard, A., Kusk, A., Merryman Boncori, J. P., Dall, J., Mankoff, K. D., Ahlstrøm, A. P., Andersen, S. B., Citterio, M., Karlsson, N. B., Kjeldsen, K. K., Korsgaard, N. J., Larsen, S. H. & Fausto, R. S. Greenland ice velocity maps from the PROMICE project. *Earth System Science Data* **13**, 3491–3512 (2021).

Methods

UAV technology

Crewed aircraft have been used previously to study fjord conditions by employing expendable CTD (also referred to as XCTD) instruments [30, 7, 32]. However, the method is constrained by aircraft hire and equipment replacement, as well as the fact that precise deployment within narrow openings in fjord ice is challenging. To alleviate these issues, we developed a novel UAV solution (Fig. 2). A complete description of the UAV, including hardware description, cost overview, and assembly and deployment instructions, is available in [28].

The UAV is based on a modified Align Trex 650X kit helicopter with an autopilot system and a custom payload attached. The autopilot provides autonomous flight capabilities and pilot assistance when manually operating the UAV. The UAV payload consists of a SonTek CastAway CTD sensor, a winch unit, and an HD camera attached to a gimbal. The Herelink HD Video system handles control, telemetry, and video transmission and has a tested range of 6 km. The winch unit consists of a winch motor that reels the CTD in and out and a pivot mechanism. This mechanism transitions the sensor from horizontal during takeoff, cruise, and landing to vertical during profiling. Once vertical, the winch motor lowers the CTD. A range of servo motors is used to control the pivot mechanism and gimbal and to engage and disengage the winch motor for the different stages of operation. The maximum measurement depth is 100 m, and a complete CTD profile (downcast and upcast) takes less than 10 minutes. The complete system is powered by a 22.2 V 14 Ah lithium polymer battery pack, which is insulated and preheated before deployment to improve performance in cold environments.

The takeoff weight of the complete UAV platform is 6.5 kg with a length of 1.145 m and a rotor diameter of 1.455 m. The maximum tested cruise speed is 16 m s^{-1}. The UAV has been tested in wind speeds of up to 7 m/s with minimal effect on performance. All components, including batteries, controller, and CTD payload, can be packed in a 1.400x450x250 mm Zarges box for shipping and handling. During fieldwork, the UAV was transported inside the cabin of an AS350 helicopter, which had two crew members and three passengers. The total cost of the UAV platform with the CTD sensor is €13,000.

Basal melt estimate

The basal melt estimate presented here stems from already published data [23] based on methods developed in [35]. We briefly summarise the methods here and refer readers to the original study for more details. The basal melt rates b_m are derived from estimates of available heat sources (E)

$$b_m = E/(\rho L)$$

Where ρ is ice density, and L is the latent heat of fusion. In the absence of surface melt, the basal meltwater is generated by friction heat and the geothermal flux [35]. Using subglacial drainage catchments delineated by the hydropotential gradients [59] (calculated from surface and bed topography from BedMachine v5 [27]), the basal melt is routed to the front of the glacier. Results show that the

average monthly basal melt volume in March is 3.8×10^6 m^3 (2010-2020 averages) [23]. This assumes that all melt generated at the bed is immediately transported to the front of the glacier and does not account for the possibility of subglacial storage or delays in subglacial transport efficiency. The uncertainty of the estimated basal melt is 21%, which stems from the fact that the basal conditions of the Greenland ice sheet are widely unknown. The uncertainty encompasses the poorly constrained geothermal flux, the frictional heat derived from ice-flow models using simplifying assumptions, and the unknown subglacial water routing (see [35]). In Fig. S1, we compare the basal meltwater volume to the surface meltwater volume. The uncertainty of surface meltwater estimate is 15%. It relates to the inherent uncertainty in the regional climate model but also to the uncertainty in the delay between meltwater production on the ice sheet and the discharge of the water at the margin, and the delineation of drainage basins that determines the water routing (see [26] for details).

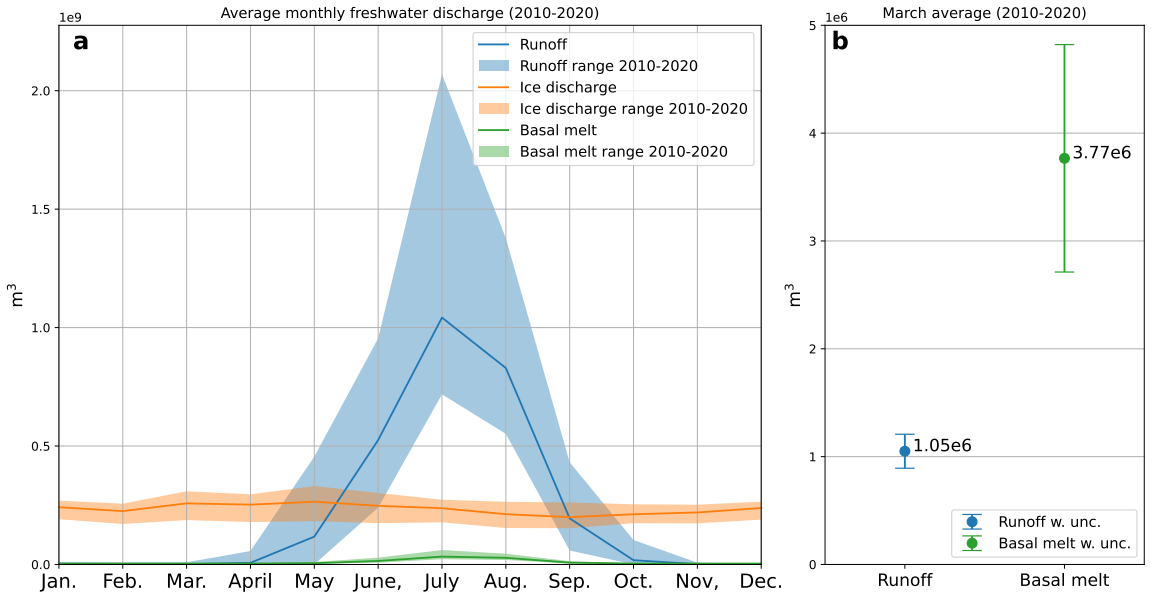

Figure S1: *Average monthly freshwater fluxes for Eqalorutsit Kangilliit Sermiat 2010-2020 [23]. In (a) the shaded areas indicate the range of values from 2010-2020. In (b) error bars show the uncertainty associated with the average values for runoff and basal melt for March.*

Estimates of surface runoff

The winter surface melt at elevations 280 m, 600 m and 900 m was estimated using an improved Positive Degree Day (PDD) model that accounts for the time lag in the melt that occurs when the air temperature is above 0°°C while the temperature of the ice surface is not yet at the melting point [36]. We combine the model with measurements from the PROMICE AWSs QAS_L, QAS_M and QAS_U [37, 60] (see Fig. 1). The improved PDD model uses ice surface temperatures to estimate surface melt rates. Here, we input measured ice surface temperatures from the AWSs, when measurements are available, or 2 m air temperatures, if ice surface temperatures are unavailable. During the period of interest, air and ice surface temperature measurements are available from the AWSs at

280 m and 900 m elevation. There are no ice surface temperature measurements from the AWS at 600 m elevation, so we estimate the ice surface temperature using measured air temperatures from the same AWS. We use a simple linear regression model trained on earlier measurements of air and ice surface temperature. A simple validation of the linear regression model indicates that the linear regression performs well with a Mean Squared Error of 1.16°C and an R-squared value of 0.97. The AWS are situated 80km west of our study area. We investigate how representative the AWS measurements are for our site by analysing the output from the Copernicus Arctic Regional Reanalysis (CARRA) model [61]. In the Supplementary Materials, figures show the 2-metre air temperatures from CARRA on a three-hour basis retrieved at grid points close to the AWS and from three elevation ranges on Eqalorutsiit Kangilliit Sermiat as shown on the maps. Also shown are the temperatures from the AWS QAS_L, QAS_M and QAS_U on daily and hourly resolution. As seen in the figures, the CARRA air temperatures agree between the two sites, with a slight tendency for faster air cooling at Sermilik Bræ between the 4th and 5th of March. We note that due to the spatial resolution of 2.5 km of the CARRA output, the elevations of the CARRA grid points do not necessarily represent the exact altitude which will influence the temperature. We also note that the AWSs generally measure lower temperatures than CARRA predicts. Finally, surface runoff estimates from CARRA (not shown) indicate zero surface runoff despite the warmer model temperatures. This gives us further confidence that we are not underestimating the surface runoff using the improved PDD model.

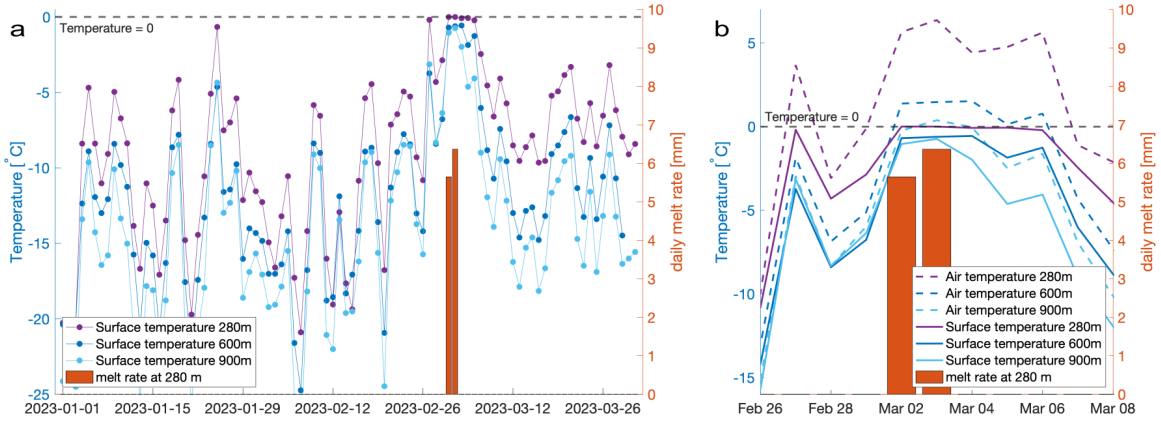

Figure S2: *Temperature time series at elevations 280 m, 600 m and 900 m by AWS approx. 80 km west of Eqalorutsit Kangilliit Sermiat and the modelled daily melt rate [36]. (a) Time series from 2023-01-01 to 2023-04-01 (b) Zoom of (a) during the high-temperature period at the beginning of March 2023 with air temperatures included.*

We use the improved PDD to estimate surface melt based on the observed (for 280 m and 900 m elevations) or reconstructed (for 600 m elevation) ice surface temperatures. The results show that of the three sites, surface melt only occurs at the lowest elevation site. The melt rate at the lowest-elevation AWS is 5.6 mm/day and 6.4 mm/day on the 2nd and 3rd of March, respectively (Fig. S2). No surface melt was recorded at the AWS at 600 m or 900 m elevation. While we cannot rule out that some of the surface meltwater penetrated to the bed of the glacier and mixed with the basal meltwater, we consider this to be unlikely for the following reasons. Firstly, visual inspection of

the glacier surface during our field campaign revealed dry crevasses (Fig. S3a), icicles (Fig. S3b), refrozen puddles of water (Fig. S3c) and snow pockets on the surface (Fig. S3d); all suggesting that water forming on the surface refreezes again. Secondly, previous studies suggest that meltwater can be stored and refrozen in the weathered glacier surface and the surface snow [38]. Finally, scrutiny of remote sensing images showed no evidence of surface water transport or drainage systems.

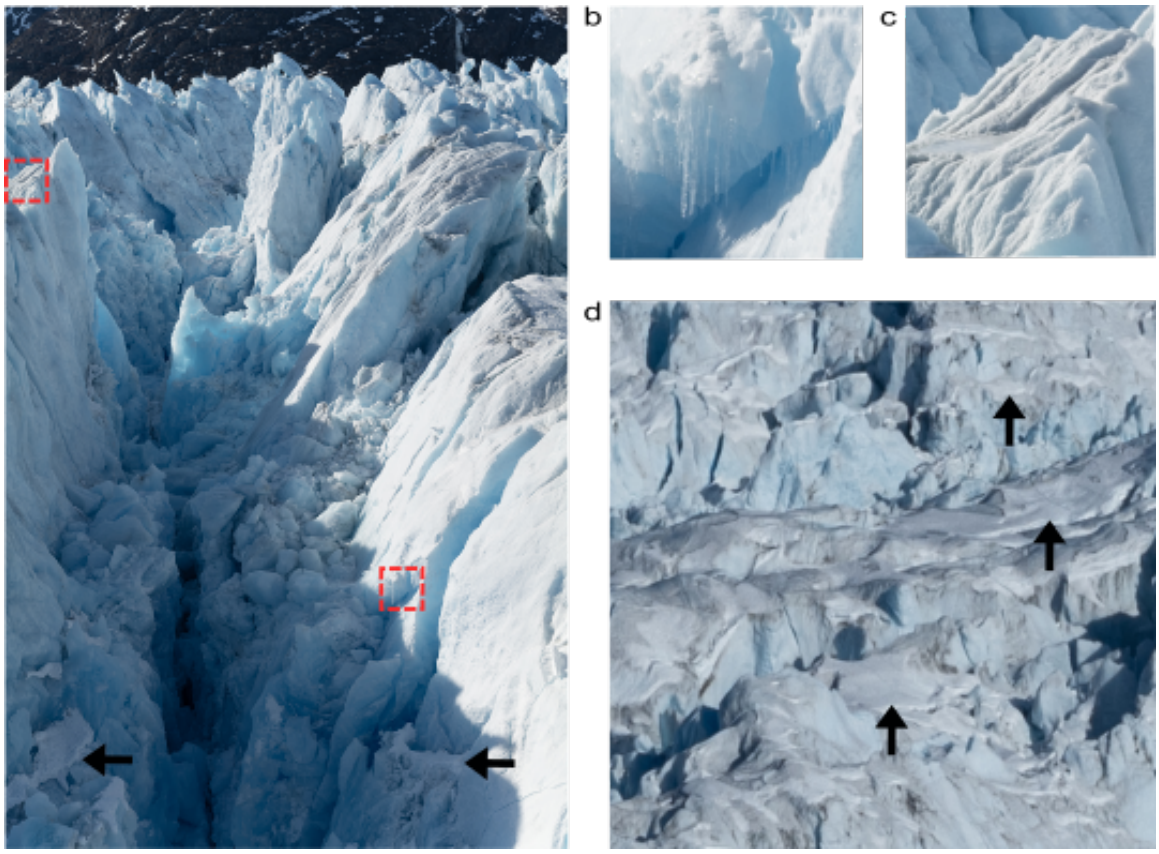

Figure S3: *Pictures of Eqalorutsit Kangilliit Sermiat taken from a helicopter by S. Rysgaard on the 27th of March 2023. (a) Crevasse photographed from the side. The red squares show the location of (b) and (c). The black arrows point to some of the snow pockets. (b) Magnification of icicles in (a). (c) Magnification of a refrozen puddle of water in (a). (d) Glacier surface photographed from above. The black arrows point to some of the snow pockets.*

Ice-marginal lake change

A time series of surface areas was derived for the five ice-marginal lakes identified between January and April 2023 (Fig. S4a). The five lakes were delineated manually across 21 timesteps using GEEDit [62]. Our dataset consists of 17 scenes from Sentinel-2 (10 m spatial resolution) and six scenes from Landsat 9 (30 m spatial resolution), and all scenes had less than 50% cloud cover (Fig. S4b). Occlusion of lake outlines occurred in some scenes due to localized cloud cover. The error estimate in lake surface area was quantified by repeated manual delineation of the Nordbosø lake

from the first Sentinel-2 and Landsat 9 image in the time series, returning an error estimate of ±4.5% and ±6.3%, respectively. The time series presented in Fig. S4b suggests that the five ice-marginal lakes in this region experienced limited variability in the areas between January and April 2023. There is no evidence of any glacier lake outburst flood or full drainage events from the five lakes. The highest value in surface lake area is evident at the beginning of the time-series record, which likely reflects the high snow cover at the start of the year. Generally, the variability in lake areas is low in the latter half of the time series, coinciding with higher data coverage, particularly from the Sentinel-2 record. The smaller lakes exhibit small changes across the time series; for example, Lake 1644 had a mean surface area of 0.23 km^2, varying between 0.19 km^2 (Sentinel-2 delineation) and 0.29 km^2 (Landsat 9 delineation), and a standard deviation of 0.03 km^2. Nordbosø Lake (lake ID 1897) exhibits the largest changes, primarily reflecting its size relative to the other lakes presented here. Lake area was stable and consistent during our field campaign and the month preceding, with an average standard deviation of 0.062 km^2 in March (compared to an average standard deviation of 0.166 km^2 over the entire time series). Thus, we conclude that there is no evidence of ice-marginal lake drainage in our study area.

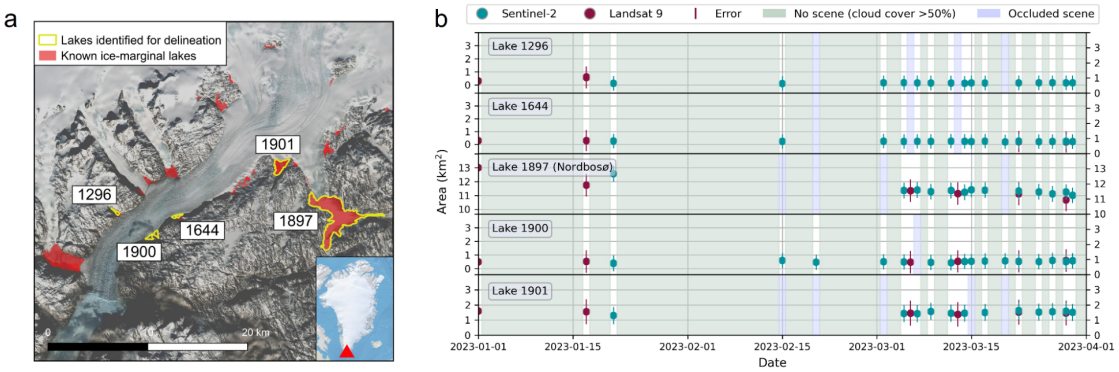

Figure S4: *(a) The five ice-marginal lakes identified between January and April 2023 within the Eqalorutsit Kangilliit Sermiat catchment area and (b) the corresponding time-series of lake area change from Sentinel-2 and Landsat 9 imagery. Known ice-marginal lakes and lake identification numbers follow those defined by the 2017 inventory of Greenland ice-marginal lakes [44]. The background image in (a) is a visible composite from Sentinel-2 imagery captured on 6th March 2023.*

Freshwater pool extent and volume

We estimate the size of the under-ice freshwater pool by assuming that the pool extends across the entire glacier front but does not extend to St. 3. We base this assumption on the fact that we did not observe any sign of subglacial discharge at St. 3. Thus, the lake must be situated between St. 3 and the glacier front, and our suggested outline indicates a likely maximum extent. The size of the pool is outlined in Fig. S5 and estimated at 14 km^2 area. Assuming that the under-ice lake has uniform salinity conditions similar to those measured at St. 1 and St. 2, we can calculate the amount of freshwater by integrating the difference between the average salinity profile of St. 1 and

St. 2 and the average salinity profiles from St. 3 and St. 4 down to 32 m depth where profiles connect (Fig. 4). The under-ice lake freshwater reservoir amounts to 2.38×10^5 m^3, an order of magnitude smaller than the theoretically estimated monthly subglacial discharge due to basal melt.

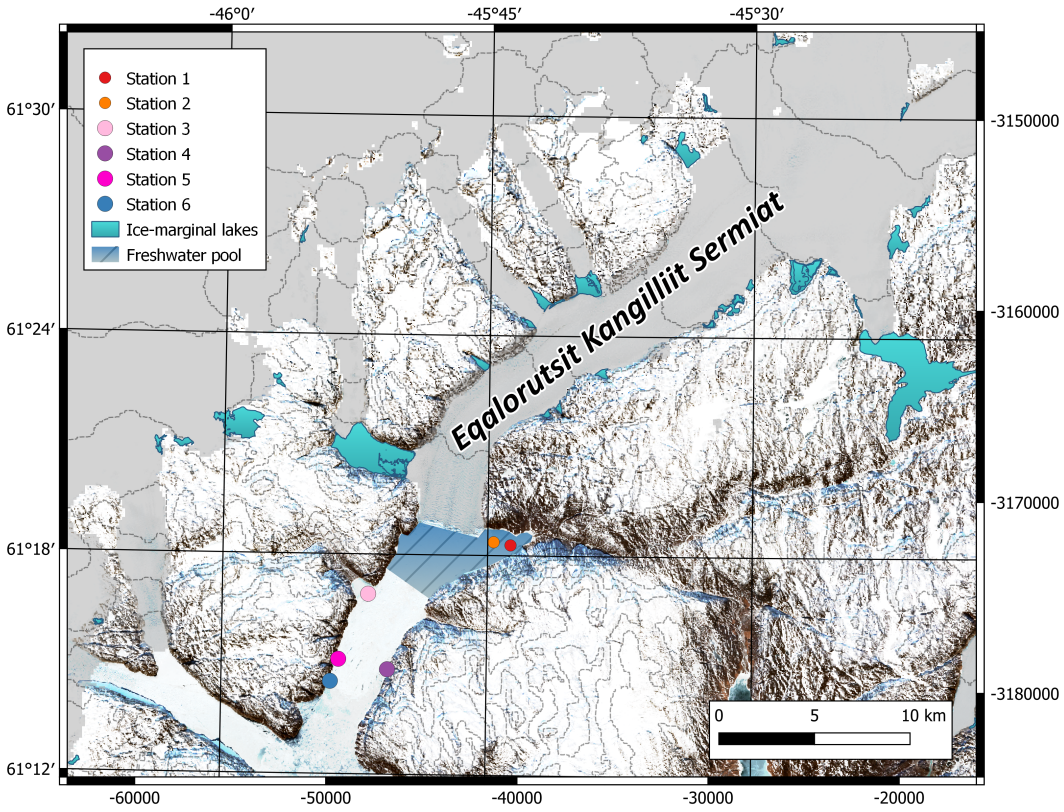

Figure S5: *Map of Eqalorutsit Kangilliit Sermiat and surrounding areas. The suggested extent of the under-ice freshwater pool is indicated in dashed blue.*

In addition to this estimate, we also investigated whether a numerical model developed for summer plume studies [47] could be used to assess the volume of the freshwater pool. In brief, we conclude that the model is not suited for our purposes partly due to the fact that it does not account for freshening caused by icebergs and ice mélange, and partly due to the fact that our measurements do not cover the entire depth of the glacier front. This is further described in the Supplementary Materials.

Data availability

The measurements acquired in March 2023, the GINR measurement KR23034, the data acquired in Nuup Kangerlua (GF10099), the estimates of ice-marginal lake extent (Fig S4) and high-resolution versions of the photos presented in Fig. S3 are available at the GEUS Dataverse DOI: 10.22008/FK2/UHV7FF. The data shown in Fig. S1 can be found at DOI: 10.22008/FK2/BOVBVR/6SU1Y6 while the AWS

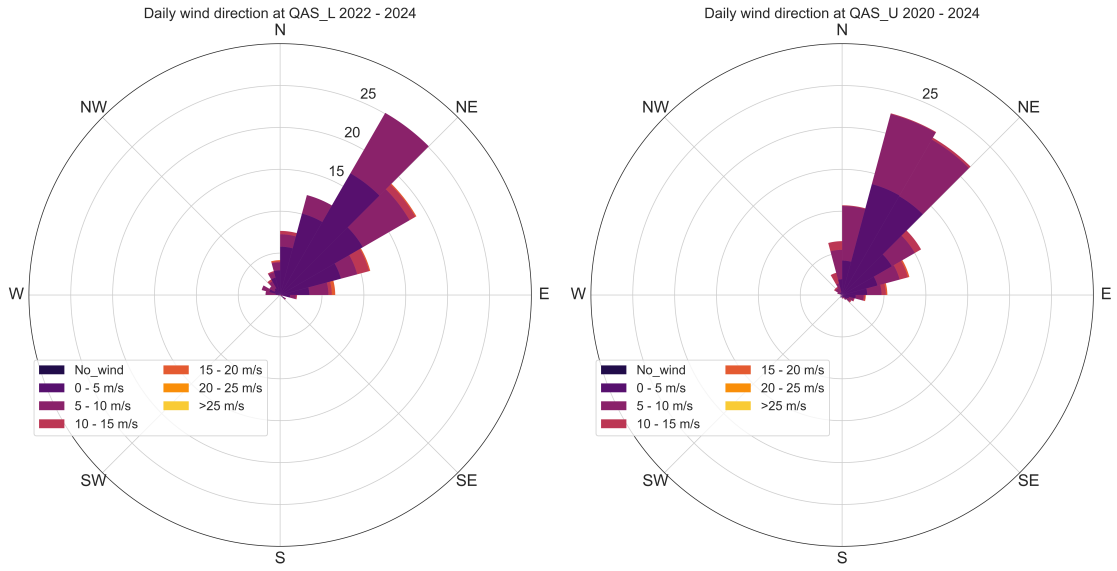

Figure S6: *Measured daily wind directions from QAS_L and QAS_U from 2022 to September 2024. As shown, the prevailing wind direction is from the northeast.*

data in Figs. S2 and S6 are available at https://doi.org/10.22008/FK2/IW73UU.

References

[59] Shreve, R. L. Movement of Water in Glaciers. *Journal of Glaciology* **11**, 205–214 (1972).

[60] How, P., Abermann, J., Ahlstrøm, A., A.P., S.B., B., J.E., Citterio, M., Colgan, W., Fausto, R., Karlsson, N., Jakobsen, J., Langley, K., Larsen, S., Lund, M., Mankoff, K., Pedersen, A., Rutishauser, A., Shields, C., Solgaard, A., van As, D., Vandecrux, B. & Wright, P. PROMICE and GC-Net automated weather station data in Greenland (2022).

[61] Yang, X., Nielsen, K. P., Amstrup, B., Peralta, C., Høyer, J., Englyst, P. N., Schyberg, H., Homleid, M., Køltzow, M. O., Randriamampianina, R., Dahlgren, P., Støylen, E., Valkonen, T., Palmason, B., Thorsteinsson, S., Bojarova, J., Körnich, H., Lindskog, M., Box, J. & Mankoff, K. C3S Arctic regional reanalysis – Full system documentation. Tech. Rep., Copernicus Climate Change Service (2021). URL `https://datastore.copernicus-climate.eu/documents/reanalysis-carra/CARRAFullSystemDocumentationF` Last accessed 23 September 2024.

[62] Lea, J. M. The Google Earth Engine Digitisation Tool (GEEDiT) and the Margin change Quantification Tool (MaQiT) – simple tools for the rapid mapping and quantification of changing Earth surface margins. *Earth Surface Dynamics* **6**, 551–561 (2018).